Physical properties of heteroatom doped graphene monolayers in relation to supercapacitive performance

Bharti[a,b], Arzu Karayel[c], Meenal Gupta[d], Gulzar Ahmad[a], Yogesh Kumar[e*] & Shatendra Sharma[f]

[a]Department of Physics, Mewar University, Gangrar, Chittorgarh-312 901, Rajasthan, India

[b]Department of Physics, Shivaji College, University of Delhi, New Delhi- 110 027, India

[c]Department of Physics, Faculty of Arts and Sciences, Hitit University, 19030,Corum, Turkey

[d]School of Basic Sciences and Research, Sharda University, Greater Noida-201 306, India

[e]Department of Physics, ARSD College, University of Delhi, New Delhi- 110 021, India

[f]School of Engineering and USIC, Jawaharlal Nehru University, New Delhi-110 067, India

Electrodes fabricated using graphene are quite promising for electric double layer capacitors. However graphene has the limitations of low 'Quantum Capacitance (QC)' near fermi level due to the presence of Dirac point that can be modified by doping graphenewith suitable dopant. The density functional theory DFT calculations are performed for doped graphene using Boron, Sulphur and phosphorus as dopants to improve the quantum capacitance of electrodes fabricated using graphene. The calculations are performed at temperatures of 233, 300 and 353 °K. From present calculations no significant temperature dependence of quantum capacitance is observed, however a marked increase in QC of value above $58\mu Fcm^{-2}$ is seen. Forphosphorus and Sulphur doped graphene a significant energy gap shift of ~ 1.5 eV from the Fermi level is observed that significantly increases the QC at Fermi level to a high value of ~ 35 μFcm^{-2}. With boron dopant as well, a shift of energy gap ~ 1.25eV from the Fermi level is observed. The shift in Dirac point increases quantum capacitance at Fermi level that in turn can increase the energy density of supercapacitor remarkably. The effect of increasing doping concentration on quantum capacitance is also investigated. These results suggest that doping of graphene may result in significant increase in QC near Fermi level, if the dopants are selected carefully depending upon the use of graphene as a positive or negative electrode. The results of these calculations reveal that the problem of low QC of graphene in the range of interest can be addressed by modifying itssurface and structure chemistry which may increase energy density in supercapacitors.

Keywords: Quantum capacitance, Graphene, Density of States, Band Structure, Supercapacitor

1 Introduction

Electric double layer supercapacitors (EDLCs) store more energy due to their electric double layer design. The materials like activated carbon, graphene, single wall carbon nanotubes and multi wall carbon nanotubes are commonly used as electrode materials. The high electrical conductivity and enormous specific surface area of graphene makes it a suitable material for supercapacitor electrodes. The tunability of graphene's structural and chemical properties[1–5] makes its use as electrode more encouraging. However, the capacitance obtained for such devices iscritically limited by the number of electronic states available near the Fermi level, called the quantum capacitance[6–10]. Therefore, for enhancing the performance of SC, it becomes important to understand thevariations in the electronic structure of

the electrode.In EDLCs, the ions of electrolyte responds actively towards the depletion and accumulation of charge resulting in the formation of an electric double layer (EDL) at the interface of electrolyte and electrode. The presence of the EDL creates a strongelectric field at the electrolyte-electrode interface. This changes the electrode's charge distribution, creating a space-charge layer. For regular electrodes fabricated using metal, effective screening reduces the impact of this charge redistribution. But, in case of graphene-electrodes, screening is poor due to a low electronic density of states (DOS). The presence of Dirac point in the band structure of graphene results in DOS having a U - shape energy dependence with minima occurring at the Fermi level. This results in U shape bias voltage dependence for the QC. Hence quantum capacitance also has a minima at the Fermi level[11]. The quantum capacitance becomes higher at high bias voltages but

Corresponding author: (E-mail: ykumar@arsd.du.ac.in)

at lower bias voltages, which are more relevant for the EDLCs, the quantum capacitance is smaller or comparable to the classical electric double layer capacitance (C_{EDL}) for typical electrolytes[12-13]. The total capacitance C of EDLC is a resultant of the series combination of quantum capacitance and C_{EDL} and thus given as:

$$\frac{1}{C} = \frac{1}{QC} + \frac{1}{C_{EDL}}. \qquad \dots (1)$$

It is clear from the above equation that near Fermi level, graphene's semiconducting behavior can significantly decrease the total capacitance.

The lower value of the density of states results in fall of the QC at low bias voltages. Doping graphene with n or p-type impurities can result in the addition or subtraction of electrons to the DOS of the system. This may result in addition of an energy gap in pristine graphene at K point and thus shifting the DOS minima away from the Fermi level. Since the minima in the density of states moves away from the Fermi level, a significant increase in density of state near the Fermi level is observed. This results in significant increase in QC at low bias voltages.

Some early theoretical studies[14-15] on the QC of single-layer grapheme have taken the fixed-band approximation (FBA) into consideration, in which discharging or charging of electrode shifts the Fermi level. But, FBA ignores the impact of the interfacial field and assumes the distribution of net charge carriers as homogeneous.

In this paper, we have performed Density Functional Theory DFT calculations on pristine and doped monolayer arm chair structure of graphene. Quantities like band gap, chemical potential, density of states and quantum capacitance are calculated. For our calculations, Boron, Phosphorus and Sulphur are used as dopants in different doping percentages. These calculations are performed at the temperatures 233, 300 and 353 °K.

2 Methodology

The arm chair structure of graphene is built using the crystal builder of the *Quantumwise* ATK package with 44 number of carbon atoms as shown in Fig. 1(a). The pristine graphene is then doped taking elements belonging to different groups of the periodic table like Sulphur (S), Boron (B), and Phosphorus (P). Calculations for band structure and chemical potential are carried out at three different temperatures *i.e.* 233, 300 and 353 °K. Doping effect on band structure and chemical potential of arm chair structure of graphene electrodes are also investigated. For this purpose, some carbon atoms are replaced by dopant atoms as shown in Figs 1(b-d) to obtain different percentages of doping.

Calculations are done for three different doping percentages *i.e.* 2 dopant atoms in layer of 42 carbon atoms, (named as D2 where D represents the symbol of the dopant), 3 dopants in 41 carbon atom layer (named as D3) and 4 atoms in layer of 40 carbon atoms, referred as D4. The structures used to
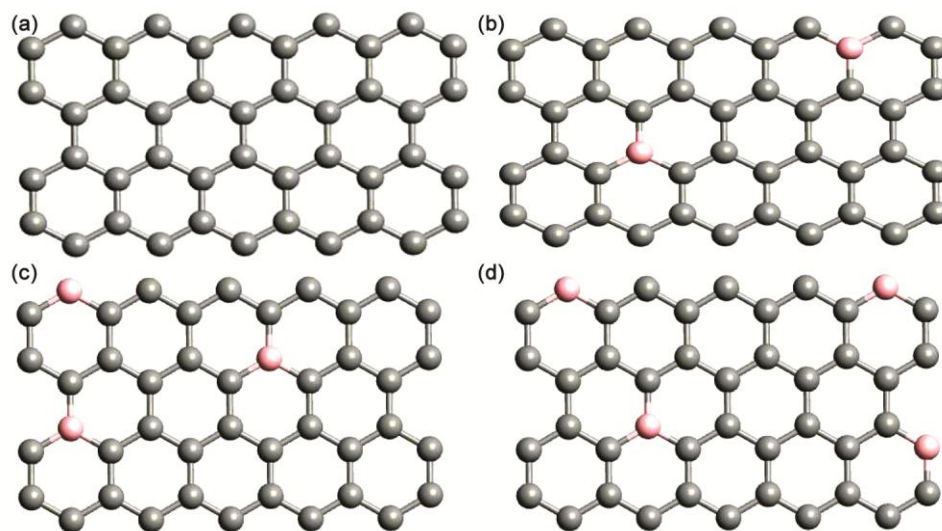

Fig. 1 — Structures used for: (a) Pure graphene, 44 carbon atoms; (b) 2 atoms of dopant and 42 carbon atoms layer *i.e.* 4.5 % doping, D2; (c) 3 atoms of dopant and 41 carbon atoms layer i.e. 6.80 % doping, D3 and (d) 4 atoms of dopant and 40 carbon atoms layer i.e. 9.1 % doping, D4

carry out the DFT calculations for given doping percentages are kept same for all the dopants. DFT Calculations are performed using the local density approximation LDA with PW exchange-correlation and Double Zeta Polarized basis set with k-point sampling at 6x6x6 grid.

For computing quantum capacitance, electrodes are modelled using first principle calculations based on density functional theory as performed in Vienna ab initio simulation package[16-18]. Projector augmented waves (PAW) is used to explain the electron-ion interactions[19-20] with plane-waves up to energy of 500 eV. The local density approximation (LDA) (CA-PZ)[21,22] is used for exchange-correlation effects. The relaxations of all structures are performed by using the conjugate gradient method. A vacuum layer of 25 Å is added to avoid interaction between neighbouring structures. After the structure optimization calculations, density of states are calculated. Then, the quantum capacitance of electrodes is calculated based on these DOS. If ϕ is the voltage applied and Q is the surface charge on graphene then from density of states at energy E (DOS(E)), we can find quantum capacitance using equations 2, 3 and 4[23-24]

$$Q = e \int_{-\infty}^{+\infty} DOS(E) \times f(E) dE \qquad \dots (2)$$

$$f(E) = \frac{1}{1+\exp\left(\frac{E}{kT}\right)} \qquad \dots (3)$$

where, *e* is the electronic charge,

E is the energy *w.r.t* the fermi energy level and $f(E)$ is the Fermi-Dirac distribution function.

By definition, one can obtain quantum capacitance by differentiating Q *w.r.t* ϕ *i.e.*

$$QC = \frac{dQ}{d\phi} = e^2 \int_{-\infty}^{+\infty} DOS(E) \times \frac{sech^2\left(\frac{E-e\phi}{2kT}\right)}{4kT} dE \qquad \dots (4)$$

Doping impacts the electronic structure of graphene. Dirac point gets shifted resulting in changes of DOS near the Fermi energy level. Due to these changes the quantum capacitance gets modified[25]. Density of states and band structure can be used to predict the nature of the charge carrier in doped graphene. In graphene, the delocalized π cloud of the pz orbitals of carbon is responsible for the density of states near Fermi level. Whereas in the doped graphene, the DOS near the Fermi level is mainly due to the dopant atoms. As QC is directly proportional to DOS near the Fermi level, tuning of the electronic structure may lead to a rise in QC values. It is expected that such results obtained theoretically by

modifying the chemistry of graphene's surface and structure may help in designing high quantum capacitance graphene electrodes.

3 Results and Discussion

Our theoretical calculations show an increase in QC for doped graphene at low bias voltages. It can be mainly due to the creation of new DOS near the Dirac point and the shift in Fermi level due to dopant atoms.The chemical potential is calculated and plotted for various doping percentages and for various dopants (Fig. 2). On doping, chemical Potential measurements exhibit a rise in the values w.r.t pristine graphene for *n*-type dopants and a fall for *p*-type at all doping percentages as seen in Fig. 2. Maximum rise in chemical potential ~27.6% is obtained for 4.5% sulphur doped graphene. The rise and fall in the chemical potential values could be attributed to the fact that doping causes a modification in the basic electronic properties of pristine graphene.

The calculations were done for three different temperatures *i.e.* 233, 300 and 353 °K. However, no impact of temperature was observed on chemical potential. The impact of different dopants and their varying percentages was studied on electronic structure and subsequently on quantum capacitance of graphene. Results show that doping can increase the QC in the low bias voltage region significantly. The increase is due to the corresponding change in the total density of states near the edges of the band. The band structure and corresponding DOS for boron doped graphene and the variation in QC with bias voltage for pristine and boron doped graphene are shown in Figs. 3-4 respectively.

In case of Boron doped graphene, with low positive bias voltages, increase in QC is seen. The increase in quantum capacitance near Fermi level w.r.t pristine graphene is higher for higher doping percentages. For negative bias voltages, QC values for doped graphene remains higher than pristine graphene for all
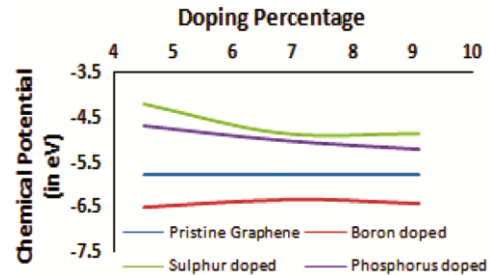

Fig. 2 — Variation of chemical potential vs doping concentration for pristine and doped graphene at T=300^{0}K
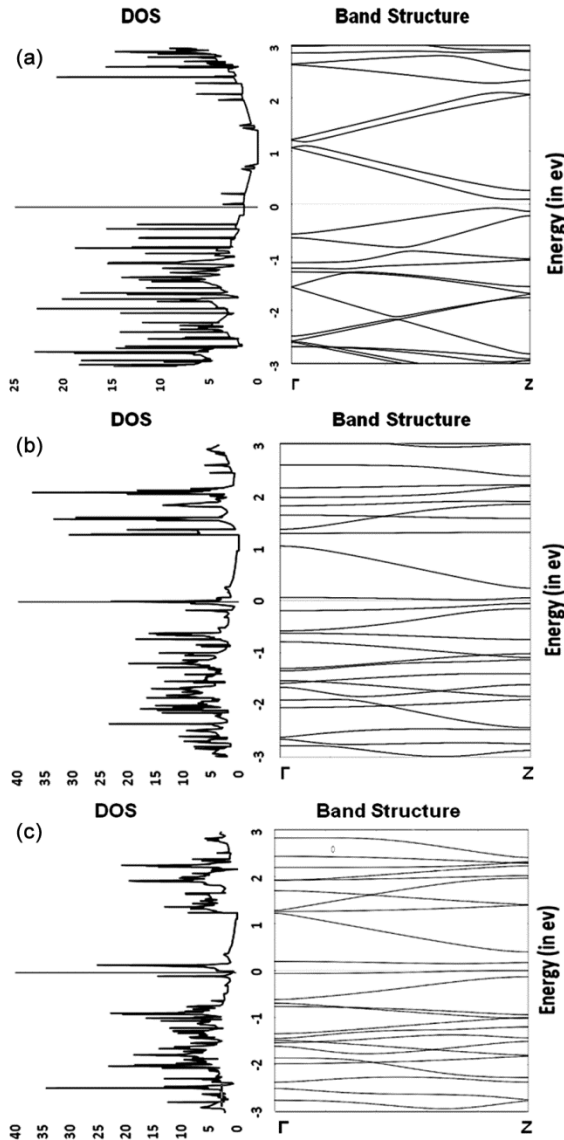
Fig. 3 — The band structure and corresponding density of states for: (a) 4.5 % B-doped graphene, B2;(b) 6.8 % B-doped graphene, B3 and (c) 9.1 % B-doped graphene, B4

values of bias voltages reaching to a maximum value of 58 μFcm^{-2} for 6.8 % doping. This can be clearly attributed to sharp increase in localized states below the Fermi level as shown in Fig. 3.

As Boron is a p type dopant *i.e.* an electron acceptor, the Fermi level of B-doped graphene shift downward into the valence band of graphene. Thus, a higher DOS can be found in the energy range between the Fermi level and −3.0 eV. Hence the QC of B-doped graphene is quite higher than that of pristine graphene in that range (Fig. 4). The values of QC with change in concentration are found to be fluctuating with bias voltage.
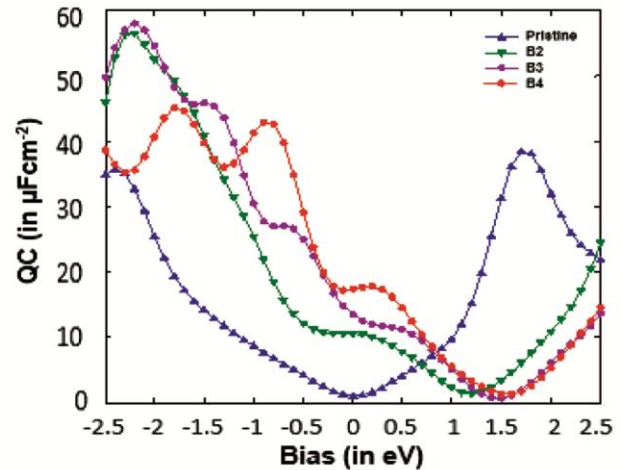

Fig. 4 — Graph obtained for variation in QC with bias voltage (for B-doped graphene with varying B/C ratios)

In case of *P*-doped graphene, since *P* is *n*-type dopant, the Fermi level of the system shifts towards the conduction band as shown in Fig. 5.

The shape of the QC profile of P-doped graphene is similar to that of pristine graphene but with the QC minima value shifted away from the Fermi level towards the negative bias voltage region as shown in Fig. 6. For low positive bias voltages (~ 1 eV), doping increases the value of QC because of higher DOS in this range but its value decreases with increase in doping percentages as shown in Fig. 6.

Highest QC of value 38 μFcm^{-2} is obtained for 4.5 % doping. One reason for the reduced QC value with increase in doping in this range is because of the interaction between the dopants in doped graphene which become much more pronounced when the dopant percentages passes the suitable value. The interactions between dopants affect the localized states near the Fermi level as can be seen in Fig. 5. As a result, the QC value decreases with increase in doping percentage. At high voltages, however, the value of QC remains lower than pristine graphene's QC because of slight decrease in DOS with increase in bias voltage from 1 to 2 eV. Although the DOS of P-doped graphene increase after the minima, the QC is still slightly lower than that of the pristine graphene in the voltage range between 1.25 and 2 eV. For negative bias voltage, QC of pristine graphene remains higher than *P*-doped graphene.

The DOS and band structures of sulphur doped graphene are shown in Fig. 7. In case of *S*-doped graphene, (Fig. 8), though the QC values are higher than pristine graphene but its variation with
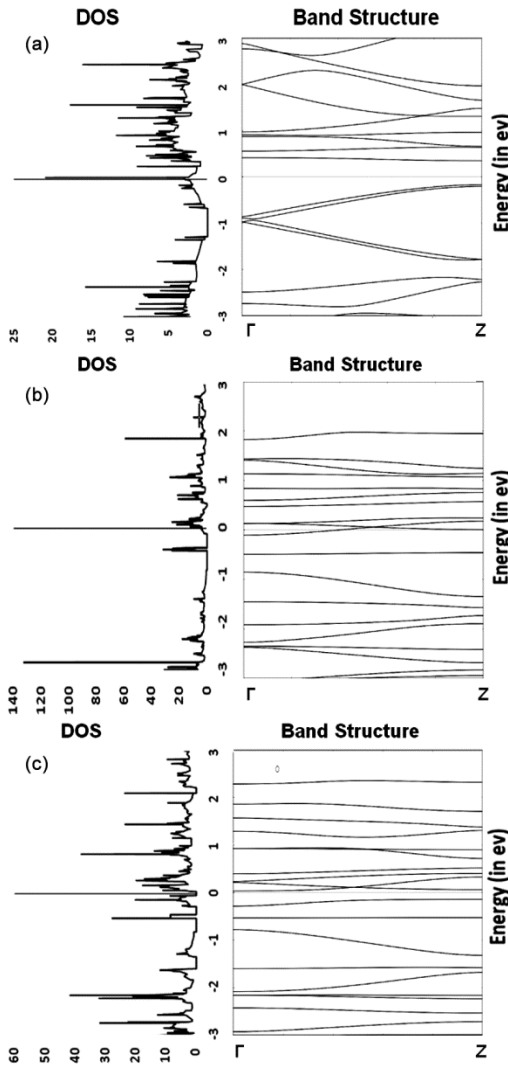
Fig. 5 — The band structure and density of states for: (a) 4.5 % P-doped graphene, P2; (b) 6.8% P-doped graphene, P3 and (c) 9.1 % P-doped graphene, P4
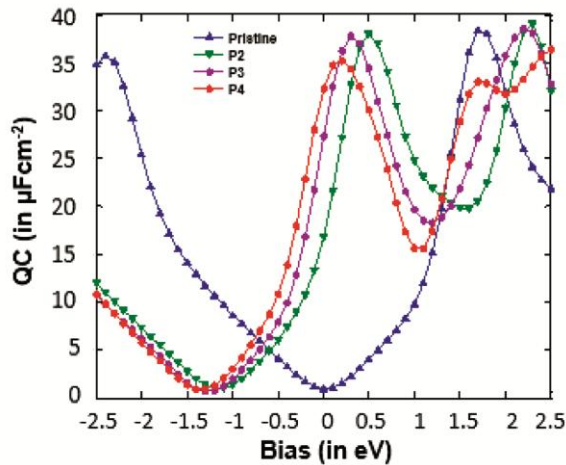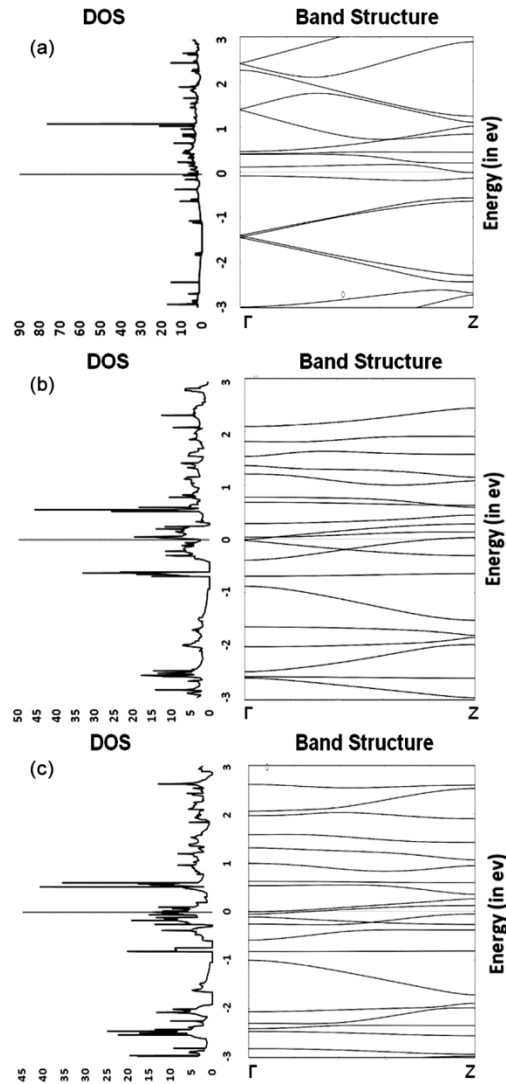
Fig. 7 — The band structure and density of states for: (a) 4.5 % S-doped graphene, S2; (b) 6.8 % S-doped graphene, S3 and (c) 9.1 % S-doped graphene, S4

Fig. 6 — Graph obtained for variation in QC with bias voltage (for P-doped graphene with varying P/C ratios)
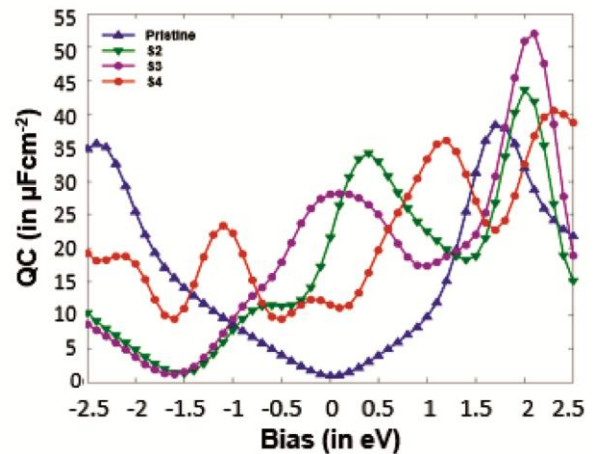
Fig. 8 — Graph obtained for variation in QC with bias voltage (for S-doped graphene with varying S/C ratios)

concentration is not as in case of *B*-doped graphene. Till 0.6 eV, QC decreases with increase in doping percentage which may be attributed to the interactions between dopant-atoms but after 0.6 eV there are fluctuations in the magnitude of quantum capacitance with doping concentration, with maximum QC ~53 μFcm^{-2} achieved for S3. QC of S doped graphene is higher than pristine graphene for negative low bias voltages also.

It appears that doping graphene with boron or sulphur increases QC near Fermi level for both positive as well as negative bias voltages. But the highest value for low positive bias is achieved with P-doped graphene. Highest value achieved for S-doped graphene is also quite close to that obtained for P-doped graphene ($\sim$ 58 μFcm^{-2}).

The findings suggest that choice of do pants for graphene used to fabricate electrodes should be asymmetric depending upon the polarity of the electrode. If graphene is to be used as anode then *n*-type dopants (S and P) should be used for doping while when used as cathode, doping with the *p*-type dopants (Boron) should be preferred. In the case of the *p* type-dopant (B atoms) the gap moves by as much as 1.25eV into the conduction band. For the *n*-dopants (P and S-atoms) the energy gap is shifted by 1.5eV into the valence band (Figs 6 & 8). Same studies were done at three different temperatures *i.e.* 233, 300 and 353 °K. No significant change is observed in the DOS profile and hence in the QC values. Similar studies done for different temperature range has also shown negligible impact of temperature on QC[11]. The QC has negligible dependence on temperature. At the Dirac point a change in temperature from 300 to 533 ^{0}K changes the QC from 0.47 to 0.95 μFcm^{-2} which is expected from the Fermi-Dirac distribution[11]. Above the $\pm$0.1 eV gate voltage the QC becomes essentially independent of temperature. Temperature stability of QC makes doped graphene based super capacitors practically viable.

4 Conclusions

The present DFT calculations of doped graphene with various dopants at different temperatures show no temperature dependence of band structure, chemical potential and DOS resulting inno significant impact of temperature on quantum capacitance. A viable method to increase QC near fermi level of graphene-based electrode materials by using DFT calculations is suggested. Graphene's electronic structure changes remarkably due to the presence of dopants B, S and P.

For positive bias voltage, the highest values of QC above 53 μFcm^{-2} is obtained for 6.8 % S-doped graphene and above 58 μFcm^{-2}for negative bias in case of 6.8 % B-doped graphene. The results obtained show that in low bias voltage range, QC of graphene can be increasedbyadding B, S and P as dopants. For Boron dopant, with positive bias, QC increases with increase in dopingconcentration. The effects of the variation of doping concentration of P and S on the increase of QC of graphene are also investigated. For low positive bias voltages, QC decreases with increase in doping concentration of P and S. The doping of graphene with boron increases QC for both positive as well as negative bias voltages. But the highest value near fermi level is achieved with *P*-doped graphene.

References

1   Biener J, Stadermann M & Suss M, *Energy Environ Sci*, 4 (2011) 656.
2   Frackowiak E, *Phys Chem Chem Phys*, 9 (2007) 1774.
3   Zhai Y, Dou Y & Zhao D, *Adv Mater*, 23 (2011) 4828.
4   Pandolfo A G & Hollenkamp A F, *J Power Sources*, 157 (2006) 1.
5   Wang DW, Li F & Liu M, *Chem Int Ed*, 47 (2008) 373.
6   Barbieri O, Hahn M, Herzog A & Kötz R, *Carbon*, 43 (2005) 1303.
7   Shao L H, Biener J & Kramer D, *Phys Chem Chem Phys*, 12 (2010) 7580.
8   Gerischer H, *J Phys Chem*, 89 (1985) 4249.
9   Stoller M D, Magnuson C W & Zhu Y, *Energy Environ Sci*, 4 (2011) 4685.
10   Wood B C, Ogitsu T, Otani M & Biener J, *J Phys Chem C*, 118 (2014) 4.
11   Vatamanu J, Ni X, Liu F & Bedrov D, *Nanotechnology*, 26 (2015) 46.
12   Druschler M, Borisenko N & Wallauer J, *Phys Chem Chem Phys*, 14 (2012) 5090.
13   Cannes C, Cachet H & Debiemme C C, *J Phys Chem C*, 117 (2013) 22915.

14   Xia J, Chen F, Li J & Tao N, *Nat Nanotechnol*, 4 (2009) 505.
15   Chen Z & Appenzeller J, *IEEE Int Electron Dev Meet*, 1 (2008).
16   Kresse G & Hafner J, *Phys Rev B*, 47 (1993) 558.
17   Kresse G & Furthmüller J, *Comput Mater Sci*, 6 (1996) 15.
18   Kresse G & Furthmüller J, *Phys Rev B*, 54 (1996) 11169.
19   Blöchl P E, *Phys Rev B*, 50 (1994) 17953.
20   Kresse G & Joubert D, *Phys Rev B*, 59 (1999) 1758.
21   Ceperley D M & Alder M J, *Phys Rev Lett*, 45 (1980) 566.
22   Perdew J P & Zunger A, *Phys Rev B*, 23 (1981) 5048.
23   Zhan C, Neal J, Wu J & Jiang D E, *J Phys Chem C*, 119 (2015) 39.
24   Yang G M, Zhang H Z, Fan X F & Zheng W T, *J Phys Chem C*, 119 (2015) 6464.
25   Elias D C, *Nat Phys*, 7 (2011) 9.